



# Edge Detection Aided Geometrical Shape Analysis of Indian Gooseberry (*Phyllanthus emblica*) for Freshness Classification

Tanmay Sarkar<sup>1</sup> · Alok Mukherjee<sup>2</sup> · Kingshuk Chatterjee<sup>2</sup> · Vladimir Ermolaev<sup>3</sup> · Dmitry Piotrovsky<sup>4</sup> · Kristina Vlasova<sup>4</sup> · Mohammad Ali Shariati<sup>4</sup> · Paulo E. S. Munekata<sup>5</sup> · Jose M. Lorenzo<sup>5,6</sup>

Received: 26 November 2021 / Accepted: 7 December 2021 / Published online: 24 January 2022  
© The Author(s), under exclusive licence to Springer Science+Business Media, LLC, part of Springer Nature 2021

## Abstract

This paper presents a freshness classification model for determining the quality of amla (*Phyllanthus emblica*) using features extracted from the progressively deteriorating shapes. Estimation of the peripheral distance from the centroid is carried out to develop key features regarding the shape of the samples, followed by developing two classifier models using support vector machine (SVM) and artificial neural network (ANN) to segment the samples into *Good* and *Deteriorated* classes. The proposed algorithm is simple in analysis as it includes geometry-based computation for identifying the surface irregularities and shape changes occurring due to aging the samples. Canny edge detection model is used to obtain the peripheral edges, followed by analyzing the same using “ConvexImage.” High accuracy of classification, exceeding 90%, is achieved in most cases, using three different feature parameters so developed, either as univariate or multivariate schemes of analysis. Besides, the sample images are captured using smartphones only. Thus, high accuracy of freshness classification, along with ease of analysis and image capturing using the phone camera itself, makes the algorithm suitable for implementing in low memory devices such as smartphones, which would also make the proposed model more widely exploring.

**Keywords** Amla · Food safety · Quality control · Canny edge detection

Tanmay Sarkar and Alok Mukherjee contributed equally

- ✉ Tanmay Sarkar  
tanmays468@gmail.com
- ✉ Alok Mukherjee  
alokmukherjee.ju@gmail.com
- ✉ Jose M. Lorenzo  
jmlorenzo@ceteca.net

- <sup>1</sup> Malda Polytechnic, West Bengal State Council of Technical Education, Government of West Bengal, 732102 Malda, India
- <sup>2</sup> Government College of Engineering and Ceramic Technology, Kolkata-700010, India
- <sup>3</sup> Department of Commodity Science and Expertise, Plekhanov Russian University of Economics, Stremyanny Lane 36, Moscow 117997, Russian Federation
- <sup>4</sup> K.G. Razumovsky Moscow State University of Technologies and Management, The First Cossack University), 73, Zemlyanoy Val St, Moscow 109004, Russian Federation
- <sup>5</sup> Centro Tecnológico de La Carne de Galicia, avd. Galicia Nº 4, Parque Tecnológico de Galicia, San Cibrao das Viñas, 32900 Ourense, Spain
- <sup>6</sup> Área de Tecnología de los Alimentos, Facultad de Ciencias de Ourense, Universidad de Vigo, 32004 Ourense, Spain

## Introduction

Due to the presence of health-boosting compositional facts like phytochemicals, vitamins, minerals, organic acids, and carbohydrates, a sharp increase in fruit consumption is perceived (Hussain et al. 2018). The consumer-driven fruit market is facing a continuous increase in requirements for higher value with respect to fruit product quality. The cutting-edge researches indicate adverse health issues are related to the consumption of spoiled fruit (Adebo et al. 2021). Thus, reliable scientific methods for on-site fruit quality evaluation is a need in recent days (Przybylak et al. 2016). The conventional fruit quality evaluations are generally offline and destructive in nature. Therefore, a rapid, non-invasive, non-contact, diverse, eco-friendly, and precise system is to be developed for fruit quality assessment (Suktanarak and Teerachaichayut 2017; Caballero et al. 2017). Digital image analysis has been used to assess the quality of agricultural produce due to its proven features like non-destructive, rapid, cost-effective, and accuracy (Ma et al. 2016; Hussain et al. 2018). Though the freshness of food materials is perspective, it regulates the consumer preference most.

Freshness depends on the variety of the fruit and on the experience of the evaluator (Koyama et al. 2021). Objective indices and consumer evaluation have been combined to follow the freshness concept in terms of consumer perception (Sarkar et al. 2021c; Koyama et al. 2021). Quantifiable standards like color, texture, and shape are performing as critical indicators during interpretation of sensory evaluation. On contrary, physicochemical characteristics could not reflect the perception of the consumers directly. Freshness prediction with sensory evaluation based on a traditional panel-based system is expensive, time-consuming, and skill-dependent, whereas machine learning-based techniques may have higher efficiency (Sarkar et al. 2021d). The classification is possibly similar to human sensory assessment without the intervention of a panelist once the model is built with an adequate dataset. The puffed snack (Sanahuja et al. 2018), fish (Dowlati et al. 2013; Liu et al. 2015), and olive oil (Angerosa et al. 1996) quality have already been evaluated with machine learning. Texture profile, sound-based sensors, and image processing have been considered to construct the predictive models. To evaluate the freshness of fruit, visual perception has been considered as most important (Péneau et al. 2007; Wada et al. 2007). Machine learning and digital image processing are in practice to facilitate food quality prediction. Smartphone-based digital image processing in combination with machine learning has been used in the freshness classification of squid and fish samples (Navotas et al. 2018; Hu et al. 2020).

Indian gooseberry (*Phyllanthus emblica*) or amla is an ethno-pharmaceutically recognized fruit from ancient times (Uddin et al. 2016). Due to the presence of the high amount of vitamin C (5–15 g/kg), emblicanin A and B, gallic acid, corilagin, quercetin, chebulagic acid, kaempferol, pedunculagin, and mucic acid, the fruit is effective in the treatment of diversified diseases, viz., cancer, neurological disorders, inflammation, indigestion, hypertension, and osteoporosis; it is a proven medicinal fruit efficacious in several infectious diseases caused by parasites and lifestyle diseases (Kapoor et al. 2020). It is a good source of dietary fiber, potassium, copper, and manganese yet low in calories, thus treated as a nutrient source for patients with diabetes, cardiovascular problems, and indigestion-related issues (Gantait et al. 2021). This seasonal fruit is available from December to March with a shelf-life of 6–9 days (Chaphalkar et al. 2017; Sarkar et al. 2021a). To get adequate nutritional features, one needs to consume fresh fruit, whereas consumption of rotten ones may initiate adverse health issues. To ascertain the freshness of the fruit changes in texture, color and shape are considered primarily (Mukherjee et al. 2021). The visual appearance followed by quality assessment is an expert-dependent attribute (Mukherjee et al. 2022).

The discontinuities within a digital image can be identified and located with the help of edge detection

(Narendra and VHareesh 2011). The discontinuity is described by an abrupt deviation in the pixel intensities to depict the object boundary in the image (Manickavasagan et al. 2014). Different edge detection techniques are there, namely, the classical, Gaussian-based, and multi-resolution methods. Edge structure, noise environment, and orientation of the edges are the variables considered for the selection of appropriate methods (Musoromy et al. 2010).

The fundamental of the SVM approach discovers the optimal separating hyperplane between classes. This may be done by observing the training cases which are present at the edge of the class descriptor. The training cases are generally known as support vectors (Bhargava and Bansal 2020). Training cases that are not included as support vectors may be discarded. This method helps to increase the efficiency of using fewer training samples as well as optimal hyperplane are also fitted. The use of small training sets leads to high classification accuracy. SVM has been used in the classification of rice and coffee bean varieties (Nga et al. 2021; Waliyansyah and Hasbullah 2021), system development for food gradation (Zhu and Spachos 2021), and carrot appearance recognition (Zhu et al. 2021).

Biological processes have been modelled reliably and efficiently with artificial neural network (ANN) for the evaluation of specific objectives (Gago et al. 2010). The arrangement and functioning of the human neural system are simulated in ANN for processing input information followed by decision-making. The non-linear and complex biological events could be modelled with ANN due to its inherent learning mechanism to establish the relationship between input and output features (Gago et al. 2010; Dutta Gupta and Pattanayak 2017).

## Materials and Methods

### Indian Gooseberry Sample Collection

Mature, excellent quality freshly harvested gooseberry (amla) fruits each having a weight of 15–21 g with a diameter of 2.6–3.5 cm were purchased from Agri Horticultural Society of India, Kolkata, India. Fifty samples had been segregated randomly out of a total of 383 samples. Emphasis has been given on reducing the time gap between purchases of amla and taking them to the laboratory; it must be within 15 min. Room temperature must be maintained at  $25 \pm 5$  °C, with a relative humidity of  $80 \pm 5\%$  (Mukherjee et al. 2021, 2022). They should not be exposed to direct sunlight and must be left without the addition of any preservatives so that natural decomposition can be observed.

## Image Acquisition

To study the decomposition rate, pictures were captured from the very first day using Redmi Note 9 Pro, with specifications 8 nm processor, 4 GB RAM, 128 GB memory, 48-megapixel camera, android system, and Samsung Isocell GM2 sensor taking view from all angles. Four LED lights were installed in the room (Eveready 20-Watt LED Battery, 20 W, 113.5 × 2.5 × 3.6 cm, luminous flux of 100 lm/W Lumen, color temperature 6000 K) to make sure there are proper lighting facilities to capture images. Fruits were placed at a distance of 20 cm from the smartphone to take images.

## Evaluation of Classes of the Fruits

Sensory qualities of the fruits were judged by a group of semi-trained panel which consisted of 39 females and 30 male persons between the age group 21 and 45 years. ISO 8586–1 (1993) was followed in performing this. On the other hand, ISO 5496:2005 and ISO 10399:2004 were employed, respectively, to identify the color and to distinguish two fruits (Sarkar et al. 2021b). Whether the fruit falls under *Good* or *Deteriorated* class is determined by three specific sensory attributes, namely, shape, color, and texture.

## Methodology of Analysis

Three major features of fruits and vegetables, which are analyzed mostly while assessing the quality of the samples, contain the color, texture, and shape of the fruits or vegetables. The proposed work is about analyzing there the shape of the amla samples. We have observed that the round-shaped amla fruits undergo an appreciable change in shape, especially, after major degradation in quality. The smooth surface of the samples mostly becomes uneven on degradation, thereby distorting the smooth and near circular peripheral

orientation. In some of the samples, we have observed that the round shape of the sample is modified close to hexagonal shape after a few days of deterioration, and other few samples trend to degrade differently in shape. Hence, a robust algorithm is required to identify these minor changes in shape. In this work, we have used the edge analysis of the samples, followed by application of the “ConvexHull” analysis to identify the exact shape of the fruits. Finally, we have computed the peripheral distance from the centroid and tried to validate the variation in these distances among the *Good* and *Deteriorated* samples using supervised learning algorithms like support vector machine (SVM) and artificial neural network (ANN). The detailed steps of designing the algorithm are started below in sequence.

## Binary Image Formation

One of the advantages of the proposed scheme is that the images need not be cropped for further analysis. Hence, the RGB images are directly converted to grayscale images in the first step of the work. We have further employed the median filtering method in order to incorporate generalization in the intensity level among the different sets of images of both *Good* and *Deteriorated* classes. Hence, we have applied median filtering over the grayscale image to obtain the median level of the images. These values are used to develop a threshold for binarizing the grayscale image itself. Hence, all the pixel intensity values belonging to higher than the threshold level are assigned as white, and values below the same are denoted as black. Thus, binary black and white images are developed from the grayscale images using the median thresholding.

Demonstration of the three different image stages of the image development, i.e., RGB image, grayscale image, and the binarized black and white image, is shown in Figs. 1 and 2. Figure 1 shows the same for a randomly chosen *Good* class of sample, whereas Fig. 2 displays the same for another randomly chosen sample from the *Deteriorated* class.

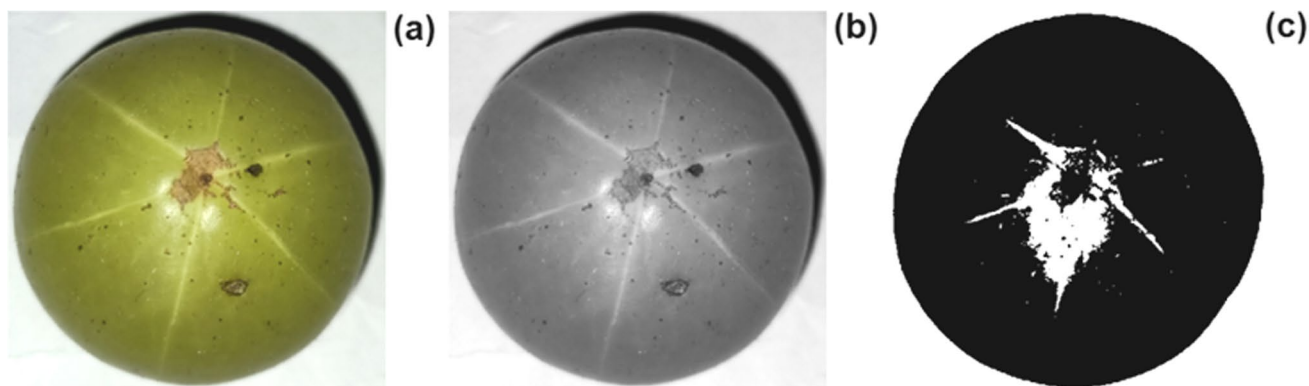


**Fig. 1** a RGB, b grayscale, and c black and white image of a random sample chosen from the *Good* class

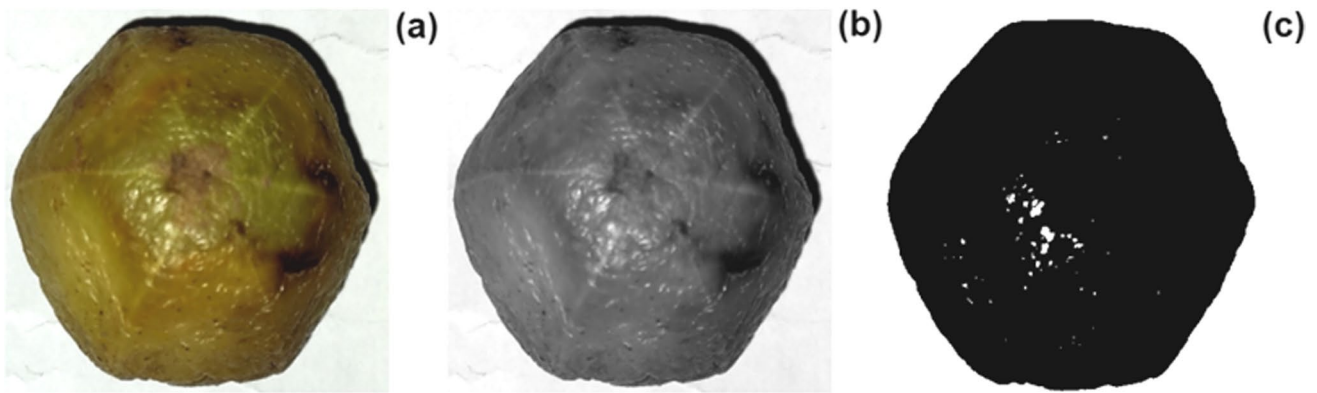


**Fig. 2** **a** RGB, **b** grayscale, and **c** black and white image of a random sample chosen from the *Deteriorated* class

**Obtaining the Edge From the Binary Image**

We have adopted “Canny” edge detection model in the proposed work, among the several variants. It is observed that there are several brownish spots all over the amla surface besides, the directly illuminated spots of the reflected light. All of these were highlighted in the black and white images and, hence, were all detected as edges, as shown in Fig. 3a and b, respectively, to demonstrate the *Good* and *Deteriorated* samples for a random sample set.

**Canny Model**

Canny (Canny 1986) introduced a very efficient edge detection algorithm by identifying the intensity discontinuities in the image. In this model, a Gaussian convolution is applied initially to the image, following a two-dimensional first-derivative operator (Hoang and Nguyen 2018). This derivative operator tries to locate the regions where there is a sharp change in intensity level between consecutive pixels, by identifying the gradient of the signal output from the

derivative function. The Gaussian filter applied initially is described as

$$g(m, n) = G_{\sigma}(m, n) * f(m, n) \tag{1}$$

where  $G_{\sigma}(m, n)$  is the Gaussian function, represented as

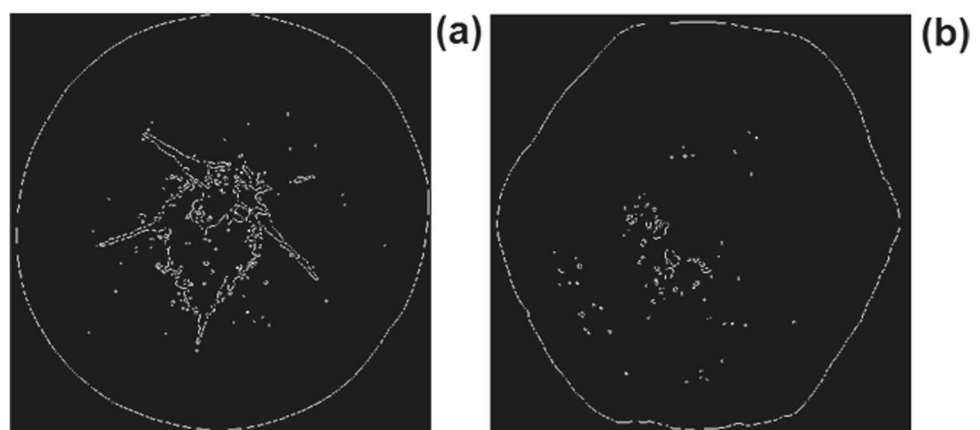
$$G_{\sigma}(m, n) = \frac{1}{\sqrt{2\pi\sigma^2}} \exp\left(-\frac{m^2 + n^2}{2\sigma^2}\right) \tag{2}$$

This function has a variance of  $\sigma^2$ , where  $\sigma$  is the standard deviation. Thus, expression (1) represents the convolution of  $G_{\sigma}(m, n)$  with  $f(m, n)$ , where  $m$  and  $n$  represent the coordinates of the image pixel location, row-wise, and column-wise and  $f(m, n)$  represents image neighborhood corresponding to pixel coordinate of  $(m, n)$ . The gradient, function  $g(m, n)$ , is computed using a certain gradient operator using the equation given by

$$g_{m,n}(m, n) = \sqrt{(g_m(m, n).N_{IC})^2 + (g_n(m, n).N_{IC})^2} \tag{3}$$

where  $N_{IC}$  represents an image neighborhood and  $g_{m,n}(m, n)$  denotes the combined result of the

**Fig. 3** Edge-detected image using “Canny” edge detection model of **a** *Good* class and **b** *Deteriorated* class



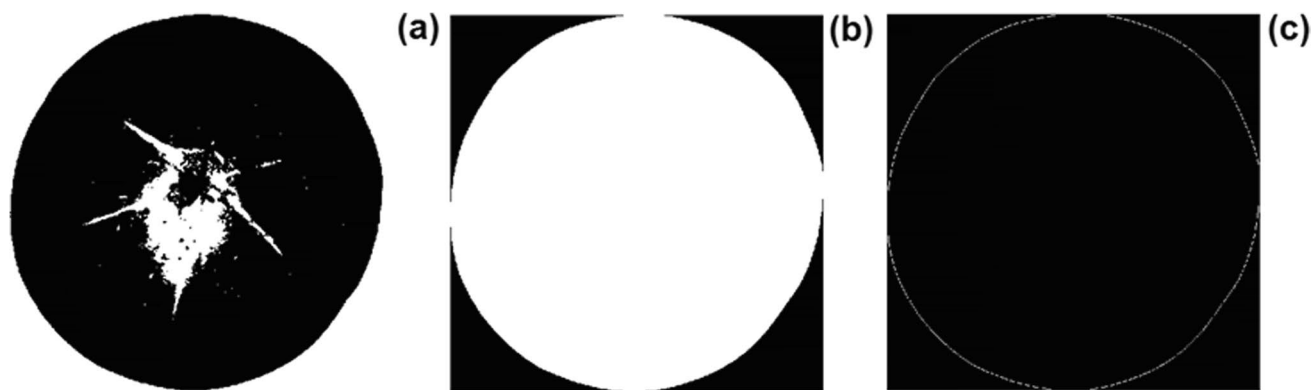


**Fig. 4** **a** Black and white, **b** “ConvexImage,” and **c** edge-detected binary image of the “ConvexImage” of a random sample chosen from the *Good* class

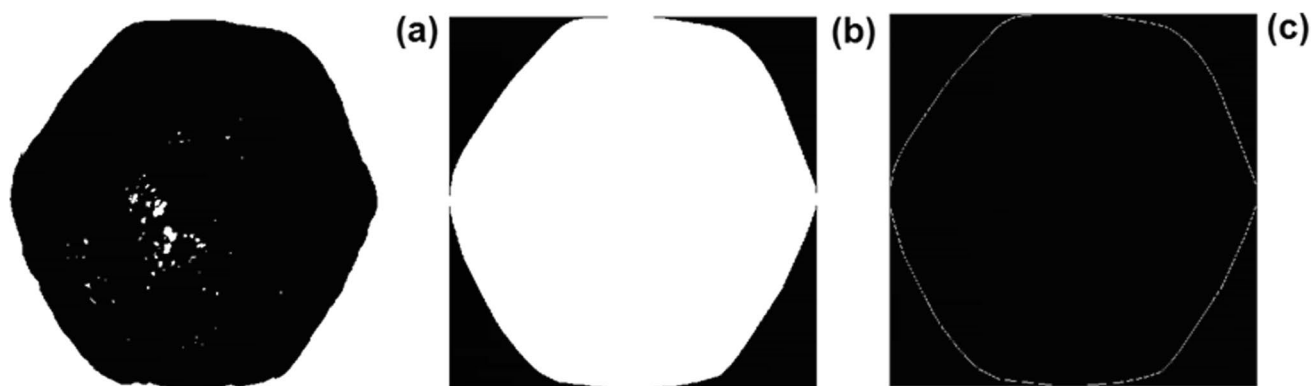


**Fig. 5** **a** Black and white, **b** “ConvexImage,” and **c** edge-detected binary image of the “ConvexImage” of a random sample chosen from the *Deteriorated* class

estimated gradients. This is followed by non-maximum suppression for narrowing out the edges (Canny 1986). The Canny model primarily relies on two specific parameters, such as  $T_1$  and  $T_2$ , which help in carrying out double thresholding analogy, where  $T_1$  is the lower threshold and  $T_2$  is the upper threshold. Hence, the edge pixels which are found higher than the upper threshold  $T_2$  are considered as strong edges, and those which are lower than the lower threshold  $T_1$  are suppressed. The edge pixels which lie in the intermediate range between  $T_1$  and  $T_2$  are also considered weak edges and primarily suppressed.

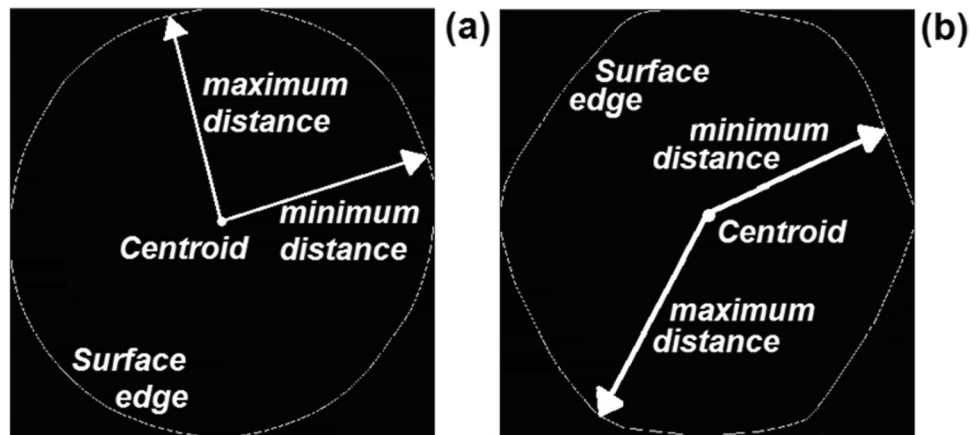
#### “ConvexHull” Analysis

The edges, which were detected within the main body of the samples, especially in more numbers in the *Deteriorated* samples, are useless for the proposed work. These edges primarily denote the illuminated spots and the brownish degradation of the fruit. In this work, we are rather concentrating more on the surface irregularities, leading to distortion

in shape of the sample. Hence, these isolated edges, detected within the fruit image, need to be eliminated for finding only the peripheral edges of the samples. In this work, we have tried to explore the peripheral surface of the samples and distinguish the deterioration for judging the smoothness of the surface. The *Deteriorated* fruits are found to have irregular and mostly hexagonal peripheral surfaces, whereas the *Good* samples have smoother and circular circumference. Hence, only the peripheral surface is required to be investigated, and the internal edges need to be removed. Thus, we have used the “ConvexHull” technique for finding out the silhouette of the amla images, which would prominently identify the irregularities on the surfaces of the *Deteriorated* samples. The method of “ConvexHull” is basically a matrix specifying the smallest convex polygon containing a particular region. “ConvexImage,” so developed from the “ConvexHull” analysis, is primarily a binary image (i.e., logical image) that specifies the “ConvexHull,” where all the pixels inside the hull are filled in, i.e., these are set on.



**Fig. 6** Computation of perpendicular peripheral distance from the centroid of the edge-detected binary image of the “ConvexImage” for a random sample chosen from the **a** *Good* class and **b** *Deteriorated* class



Two different example cases of *Good* and *Deteriorated* classes are demonstrated in Figs. 4 and 5, respectively. Figures 4b and 5b show, respectively, the “ConvexHull” of the two classes. These “ConvexHull” images are further analyzed using an edge detection model to identify the peripheral edges most prominently. The final images of Figs. 4c and 5c contain only the surface edges and disregard any of the edges developed interior to the samples, as was found on direct edge analysis of the black and white images obtained as Fig. 3a and b, respectively. This clearly demonstrates the effectiveness of the “ConvexHull” model used in the present case in connection with edge analysis.

**Computation of Peripheral Distance and Development of Feature Ratios**

The next task is the estimation of the peripheral edges from the center of the edge-detected image. Hence, we have first computed the centroid of the image along the x and y coordinates, respectively. The edge image is basically a binary image where the black pixels are denoted by zero and the white edges are denoted by unity. Thus, we have first found out the centroid of each image and then computed the Euclidean or victor distance of each of these peripheral edge pixels (denoted by intensity level 1) from the centroid.

We have observed that the *Good* class of images has a smoother peripheral surface, whereas the *Deteriorated* samples have developed several irregularities. The most important observation that we have noticed is that many of the samples, on degradation, become close to hexagonal in shape. This is due to the reason that amla has six major axes along the surface, i.e., each major axis lies close to 60° apart. The surface straightens more in between the two major axes, and hence, the shape of some of the *Deteriorated* sample closes to a regular hexagon.

The method of determining these distances is shown in Fig. 6a and b, respectively, for the *Good* and *Deteriorated* samples.

The edges obtained from these images are analyzed to find out the distances between the centroid and the peripheral edge points as discussed in the earlier section. These distances are the major features that are considered for subsequent analysis. It is well-known that when the samples are in good condition, the surface is smoother and the shape is closer to a circle, whereas when these deteriorate, the peripheral surface wrinkles and shrinks in many areas. Hence, the variation of the distance between the centroid and the peripheral point is more in the case of the *Deteriorated* samples. The same distances for the *Good* samples are very close to each other since the peripheral surface is much smoother and almost equally distant from the centroid. Thus, three ratios are developed using these peripheral distances as follows:

$$Ratio1 = (Standarddeviationofthevectordistances)/(Minimumvectordistance) \times 100 \tag{4}$$

$$Ratio2 = (Maximumvectordistance)/(Minimumvectordistance) \tag{5}$$

$$Ratio3 = (Maximumvectordistance - Minimumvectordistance) / (Minimumvectordistance) \times 100 \tag{6}$$

These features are analyzed further using support vector machine (SVM) model and artificial neural network (ANN) model to authenticate this difference in variation of the peripheral distances and thereby classifying models between the *Good* and *Deteriorated* classes. The whole method of image classification is described here using a sort of pseudo code, followed by describing the same using a flow diagram (Fig. 7).

**Algorithm:**

*/ Begin*

*/ Identifying the centroid from the 'ConvexHull' image:*

$$Cen_{x,y} = (x, y)$$

*/ Locating all the peripheral surface edge points from the image*

*Finding out the row and column indices of the pixels with non-zero values: Edge pixels*

*[Row, Col] = finding non-zero elements from 'ConvexHull' image;*

*The length of this array:[Row, Col] is variable and depends on the number of edges*

*obtained*

*/ Computation of the vector distances from the centroidDis(i) to the edge detected points*

*Repeat for i = 1 to (size of the array [Row] or [Col]) and use this expression,*

$$Dis(i) = \sqrt{(Cen_{x,y}(x) - Row_i(x))^2 + (Cen_{x,y}(y) - Row_i(y))^2} \text{ or,}$$

$$Dis(i) = \sqrt{(Cen_{x,y}(x) - Col_i(x))^2 + (Cen_{x,y}(y) - Col_i(y))^2}$$

*/ Obtaining the variable-length distance-vector array [Dis].*

*/ Further computing three detection feature parameters as:*

*Ratio 1 = (Standard deviation of [Dis]) / (Minimum of [Dis]) × multiplier;*

*Ratio 2 = (Maximum of [Dis]) / (Minimum of [Dis]);*

*Ratio 3 = (Maximum of [Dis] - Minimum of [Dis]) / (Minimum of [Dis]) × multiplier;*

*/ Design the proposed SVM and ANN classifiers*

*/ Three features are given as input to the models; both pair wise and as sole feature*

*/ Classifier accuracy predicted*

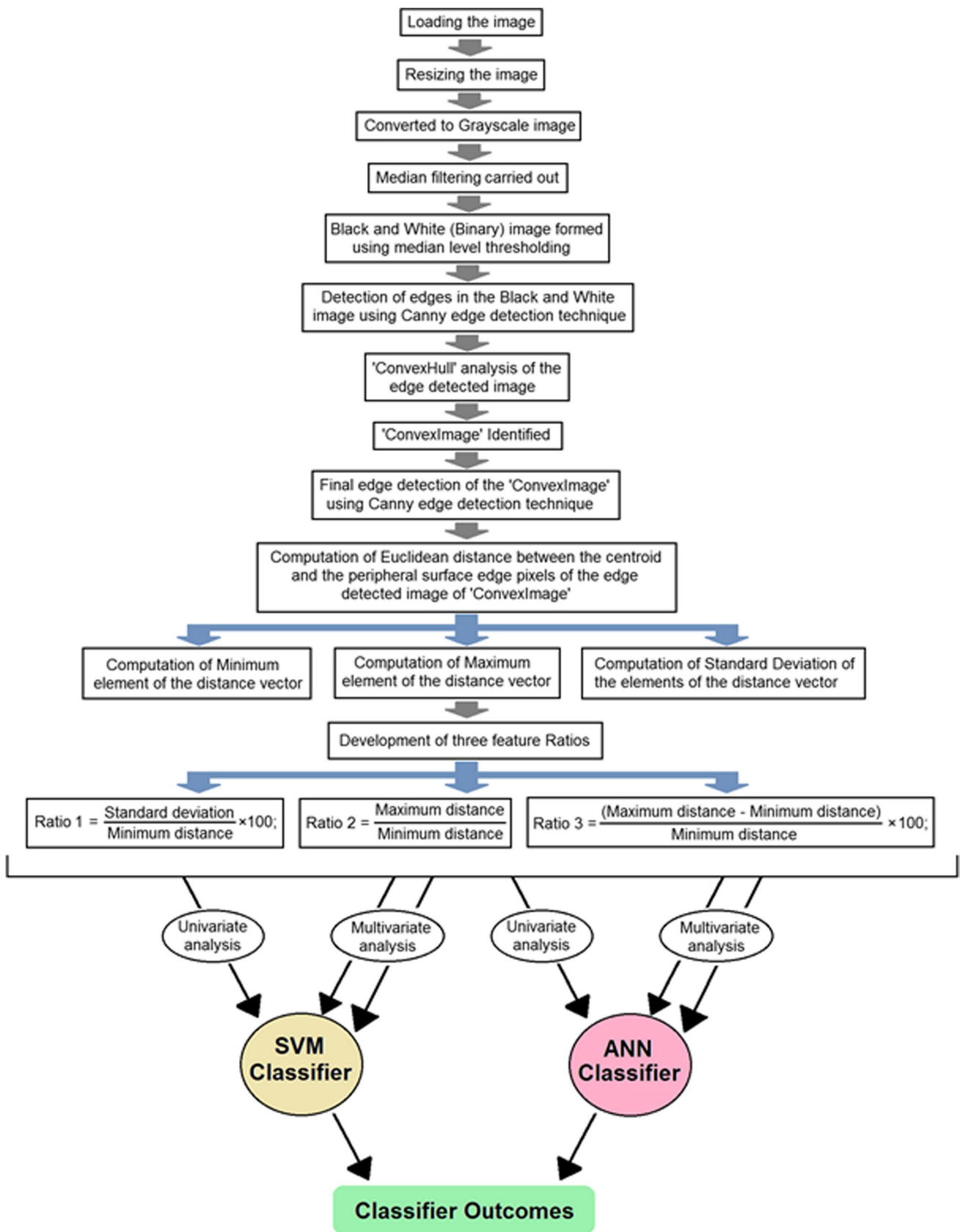


Fig. 7 Flowchart of the proposed freshness classifier



## Result and Analysis

We have studied the variations of the peripheral distance from the centroid of each edge-detected image carefully. In this work, we have analyzed 170 *Good* samples and 170 number of the *Deteriorated* samples. Results show that the variation of the peripheral distances is much higher in the case of *Deteriorated* samples compared to the *Good* ones, which is in connection with the rationale so developed. These variations of a *Good* class of sample and a *Deteriorated* class of sample, picked up in random, are shown in Fig. 8.

The blue lines which are the computed peripheral distances of a *Good* sample are observed to lie within a range, which is much lower compared to the red lines, indicating a *Deteriorated* sample. In order to quantify the same, we have analyzed the three major detection parameters from these variations, given by expressions (4), (5), and (6) respectively, which are used further with the SVM and ANN classifier models. These three ratio parameters are computed for all the samples, and the variation of these three parameters is shown in Fig. 9.

It is observed from all the subfigures of Fig. 9 that there is a visible distinction between the *Good* and *Deteriorated* samples considering all three ratios. Figure 9b and c are identically close since these two ratios are depending directly on the maximum and minimum peripheral distance from the centroid. This apparent separation of the two classes using all the three features is further analyzed graphically using boxplots as shown in Fig. 10, which further emphasizes the above facts.

These boxplots clearly show that the two classes with all the three feature ratios are separable with little overlap between the separating classes. The boxplots of ratio 2 and ratio 3 especially show that there are few outliers

that lie within the region of the opposite classes. Hence, this qualitative separation of the feature points for all the three ratios is analyzed using SVM and ANN classifiers. We have used all the three feature ratios independently in the proposed SVM classifier, as well as taken pairs of these features and plotted them against each other. The plot of ratio 1 against ratio 2 for all the samples points, including the *Good* and *Deteriorated* classes, is shown in Fig. 11a, and the contour of the points is also marked with a continuous line. Apparent observation of Fig. 11a shows that there is overlap between the two classes when observed qualitatively. Hence, these features are used with the proposed SVM classifier to develop an accurate classification of the same. The SVM classification of the whole set of samples is shown in Fig. 11b which demonstrates that the two classes of samples are well separated using a single line to yield classifier accuracy exceeding 90%.

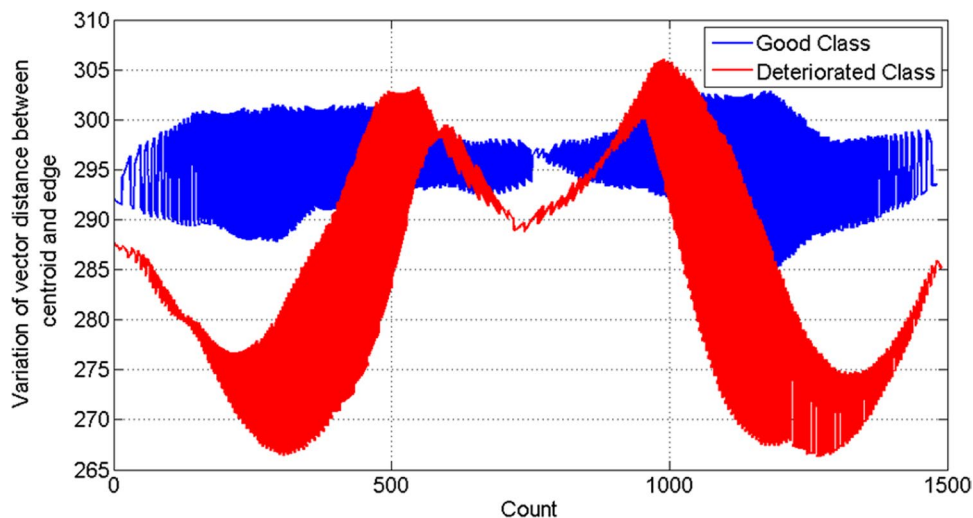
## Classifier Outcomes

The classifier outcomes using the two supervised learning models are shown in Tables 1 and 2.

It is observed from the table that the classifier accuracy, using both the SVM and ANN models, is very much comparable, including both the univariate and bivariate schemes. These results are further illustrated using bar diagram as shown in Fig. 12 and Fig. 13 to compare the classifier outputs from these two models, as well as compare the results from univariate and bivariate models.

It is further emphasized from Table 2 and from Figs. 12 and 13 that both of these models produce comparable outcomes, although SVM model possesses minor advantage over the ANN prototype in terms of marginally improved average, maximum, and the least accuracy level. This is

**Fig. 8** Variations of orthogonal distance between the centroid and the peripheral edge pixels for two randomly chosen samples; one from each of the *Good* class (shown in blue lines) and *Deteriorated* class (shown in red lines)



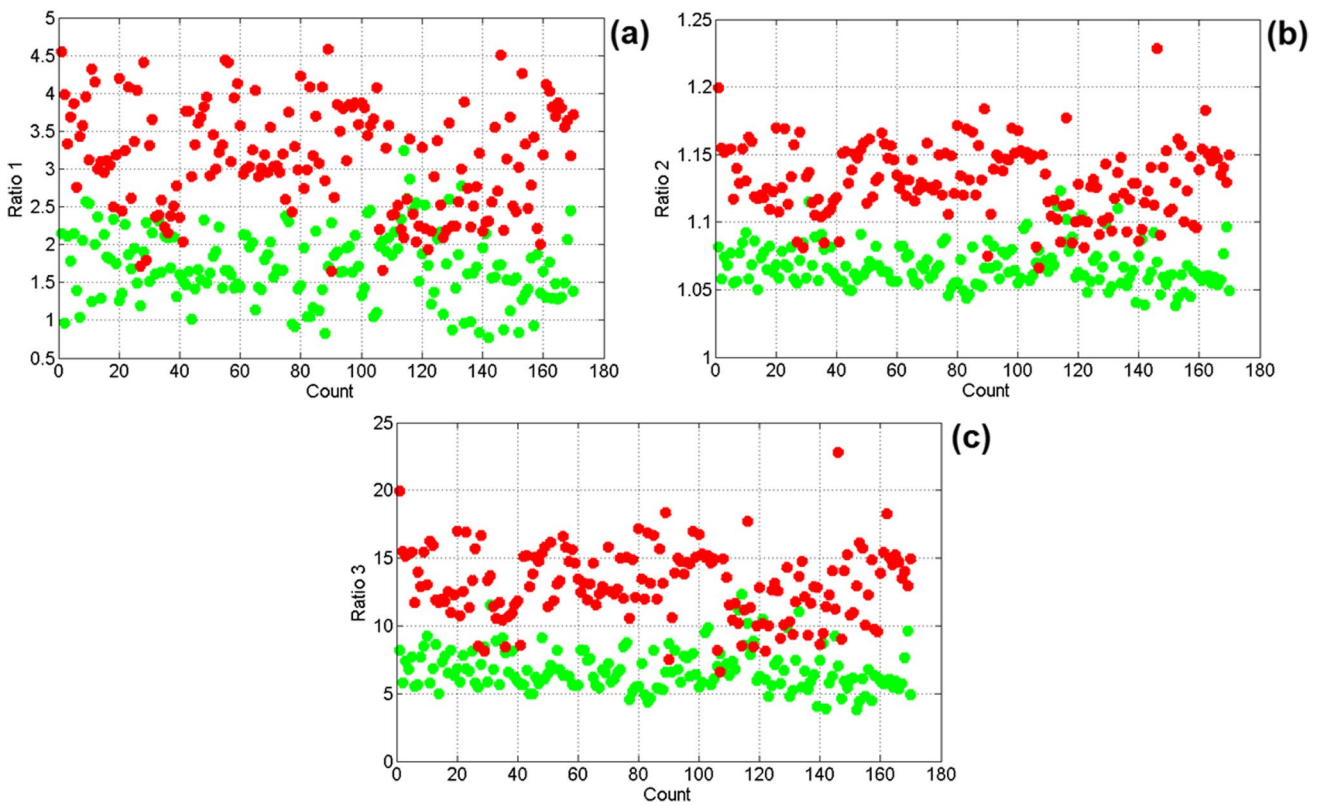
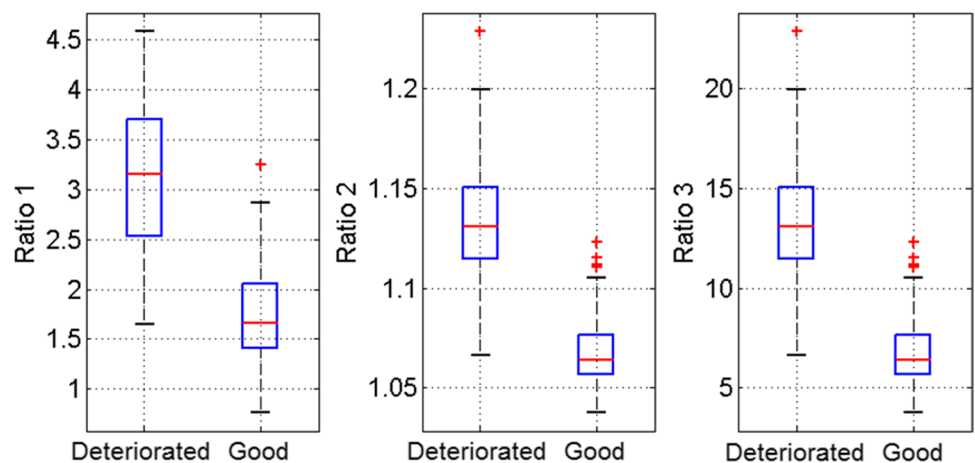


**Fig. 9** Scatter diagram of the three different feature ratio points of the 170 samples belonging to the *Good* class (shown in green circles) and 170 samples belonging to the *Deteriorated* class (shown in red circles): **a** distribution of ratio 1, **b** distribution of ratio 2, and **c** distribution of ratio 3

observed from each sub-figure of Fig. 12. But, the ANN model, although is marginally behind the SVM classifier in terms of the mean classification accuracy, has one minor advantage in terms of the average deviation in accuracy outcomes from sample to sample, which is represented by

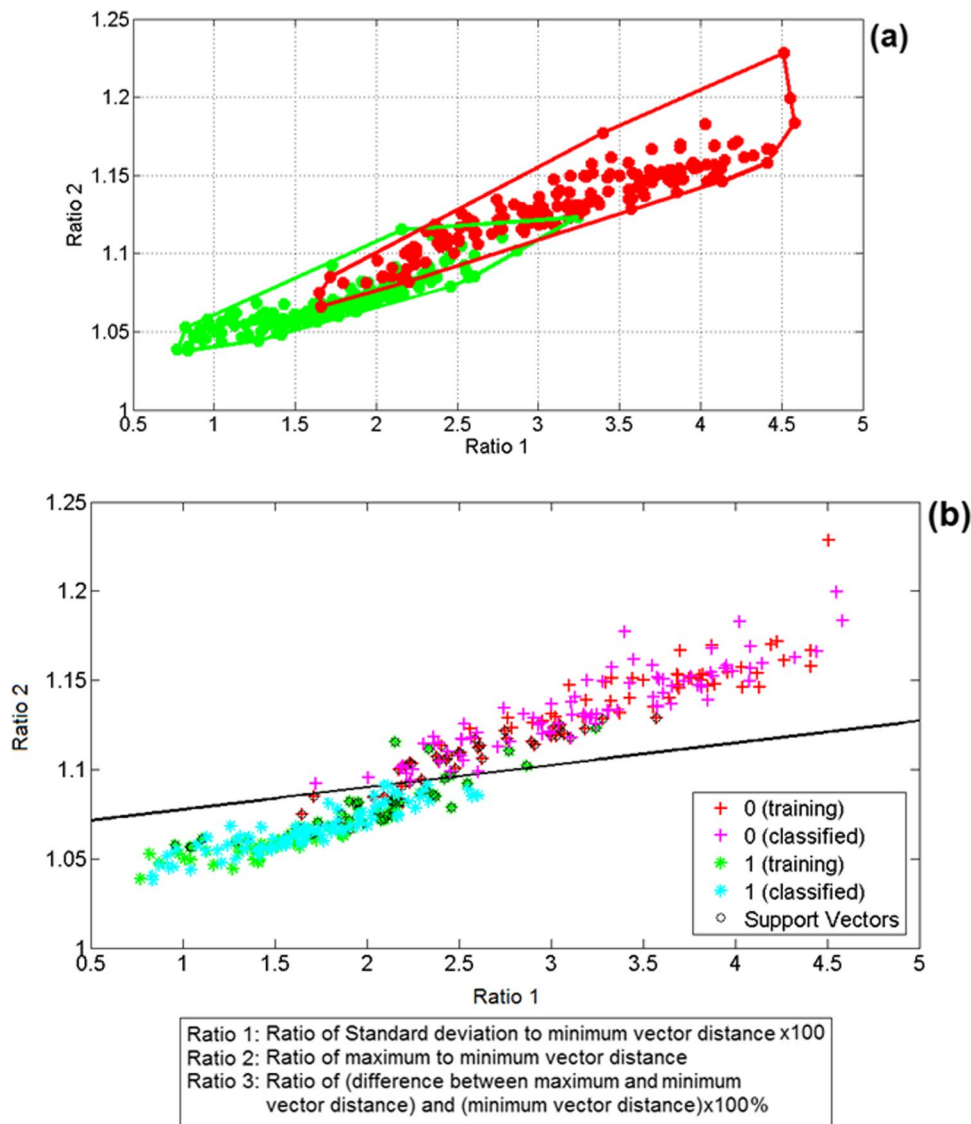
the standard deviation of the results as shown in Fig. 13a. This inference is further highlighted from the range of accuracy levels from both the models, which is described in Fig. 13b. It is well observed from this sub-figure that the range of classifier accuracy levels obtained from 50

**Fig. 10** Boxplots showing the distribution of three different ratio feature points of the *Good* and *Deteriorated* class: **a** distribution of ratio 1, **b** distribution of ratio 2, and **c** distribution of ratio 3



Ratio 1: Ratio of Standard deviation to minimum vector distance x100  
 Ratio 2: Ratio of maximum to minimum vector distance  
 Ratio 3: Ratio of (difference between maximum and minimum vector distance) and (minimum vector distance)x100%

**Fig. 11** **a** Bivariate distribution of ratio 1 and ratio 2 values of the *Good* class (shown in green circles) and *Deteriorated* class (shown in red circles), the terminal points are contoured; **b** SVM classification of the same distribution of samples



numbers of experimental observations is higher for SVM outputs in most of the cases. This further infers that the ANN classifier produces somewhat less deviation in results for consecutive experiments, although this difference is not majorly distinct.

Another comparison between the univariate and bivariate analysis schemes, using both the models, shows that the bivariate analysis produces marginally improved accuracy level compared to the univariate analysis-based models, as observed from the mean and maximum and minimum levels of accuracy plot of Fig. 12. This improvement of maximum accuracy attained using bivariate scheme is more predominant with the ANN model, as found from Fig. 12b. Thus, in a single note, both the proposed classifier models work almost equally efficiently in predicting the freshness class of the samples.

### Analysis of the Model Performance

The model performance is evaluated considering the following:

$$\text{Accuracy}(\%) = (P_{\text{True}} + N_{\text{True}}) / (P_{\text{True}} + P_{\text{False}} + N_{\text{True}} + N_{\text{False}}) \tag{7}$$

$$\text{Precision} = P_{\text{True}} / (P_{\text{True}} + P_{\text{False}}) \tag{8}$$

$$\text{Sensitivity}(\text{TPR or true positive rate}) = P_{\text{True}} / (P_{\text{True}} + N_{\text{False}}) \tag{9}$$

$$\text{Quality measure} = 2 \times (\text{Sensitivity} \times \text{Precision}) / (\text{Sensitivity} + \text{Precision}) \tag{10}$$

$$\text{Intersection of overall union} = P_{\text{True}} / (P_{\text{True}} + P_{\text{False}} + N_{\text{False}}) \tag{11}$$

**Table 1** Previous researches on edge detection techniques in the field of food analysis

Food system	Aim of research	Edge detection technique	Metrics for performance analysis	Accuracy	Reference
Egg	Detection of cracks on the surface of eggs	Sobel filter	Specificity, accuracy, false positive rate, false negative rate	94.0%	Priyadumkol et al. 2017
Red and green apple, potato, carrot, orange, mango, egg, pear	Measurement of volume of different food product	Sobel filter	Mean square error	-	Siswantoro et al. 2015
Slice of marbled meat	Estimation of fat content in meat	Canny method	Root mean square error, signal-to-noise ratio	-	Hussein et al. 2011
Milkfish, round scad, and tilapia fish	Classification of fish freshness	Canny method	Accuracy	Milkfish = 90.0% Round scad = 93.3% Tilapia = 100%	Navotas et al. 2018
Red and green apple, orange	Recognition of fruits and classification of the fruits depending on their size	Canny and modified Canny method	Accuracy	100%	Rabby et al. 2018
Litchi, mango, pomegranate, papaya, and orange fruits in the tree	Detection of fruit on the tree	Gradient magnitude	Accuracy	90.0%	Hetal et al. 2011
Apple	Detection and gradation of fruits	Connected boundary tracking method	Absolute and relative error	-	Dang et al. 2010
Olive	Defect detection and classification (healthy)	Special image convolution algorithm, texture homogeneity measuring technique, Canny method	Accuracy	65–100%	Hussain Hassan and Nashat 2019
Apple	Defect detection from thermal images	Canny method	Rate of detection	Defective and sub-surface defective = 90% Sound = 100%	Satone et al. 2017
Orange	Detection of oranges	Canny method	Accuracy	85%	Thendral et al. 2014
Rice	Grading and detection of stone in rice	Canny method	-	-	Pratibha et al. 2017
Rice	Classification on the basis of rice type and length of rice	Gradient, differentiation, Sobel, Sigma, Roberts, and Perwitt	-	-	Mahale and Korde 2014
Banana	Ripeness and size determination	Sobel, Prewitt, zero-cross method, Roberts, Laplacian of Gaussian (LoG), Canny method	-	-	Mustafa et al. 2008
Dates (Fard variety)	Hard and soft classification	Canny, LoG, Roberts, Sobel, high-pass filter	Accuracy	75–97.3%	Manickavasagan et al. 2014
Banana	Ripeness determination	LoG	Accuracy	98.0%	Mendoza and Aguilera 2004
Mango	Mango detection from video	Sobel, Prewitt, Canny	-	-	Gaikwad and Manza 2012
Indian restaurant food	Segmentation and classification of Indian cuisines	Edge adaptive deep convolutional neural network	Accuracy, sensitivity, Jaccard score	98.77–99.48%	C. Burkapalli and Patil 2020
Papaya	Fruit detection in its natural background	Canny method	-	-	Limsiroratana and Ikeda 2005

**Table 1** (continued)

Food system	Aim of research	Edge detection technique	Metrics for performance analysis	Accuracy	Reference
Potato chips	Potato chip classification based on texture and color	LoG	Accuracy	84.7%	Mendoza et al. 2007
Potato chips	Machine vision system development	LoG	-	-	Pedreschi et al. 2006
Rice	Identification of different rice variety and quality analysis	Canny method	Accuracy	Classification = 92.3% Quality = 89.5%	Asif et al. 2018
Pizza, rice, and apple	Food quality inspection	Sobel, Canny, Prewitt, LoG, Roberts, zero crossing	-	-	Narendra and VHareesh K., 2011

where:

**Table 2** Outcomes of the two-edge detection-based freshness classifier models

Classifier model	Number of variables involved	Classifier features	Classifier accuracy (%)			
			Mean	Maximum	Minimum	SD
SVM	Univariate classification	Ratio 1 only	87.2	91.2	81.8	2
		Ratio 2 only	92.2	95.3	88.8	1.3
		Ratio 3 only	92.4	95.3	88.8	1.6
	Bivariate classification	Ratio 1 and ratio 2	93	95.9	88.2	1.6
		Ratio 1 and ratio 3	92.7	95.3	88.2	1.5
ANN	Univariate classification	Ratio 2 and ratio 3	92.9	95.9	90	1.4
		Ratio 1 only	86.5	88.5	82.7	1.8
		Ratio 2 only	90.6	92.9	87.3	1.2
		Ratio 3 only	90.7	92.4	87.5	1.5
		Bivariate classification	Ratio 1 and ratio 2	92.8	95.3	88.7
	Ratio 1 and ratio 3		93.3	95.3	89.1	1.5
	Ratio 2 and ratio 3		90.1	92.7	87.8	1.3
	Multivariate classification	Ratio 1, ratio 2, and ratio 3	91.9	94.1	88.3	1.4

$$\text{Specificity (true negative rate)} = \frac{N_{\text{True}}}{(N_{\text{True}} + P_{\text{False}})} \quad (12)$$

$$\text{Negative predictive value} = \frac{N_{\text{True}}}{(N_{\text{True}} + N_{\text{False}})} \quad (13)$$

$$\text{False positive rate (FPR)} = \frac{P_{\text{False}}}{(P_{\text{False}} + N_{\text{True}})} \quad (14)$$

$$\text{False negative rate (FNR)} = \frac{N_{\text{False}}}{(N_{\text{False}} + P_{\text{True}})} \quad (15)$$

$$\text{Mathew Correlation (MC)} = \frac{[(P_{\text{True}} \times N_{\text{True}}) - (P_{\text{False}} \times N_{\text{False}})]}{\sqrt{[(P_{\text{True}} + P_{\text{False}})(P_{\text{True}} + N_{\text{False}})(N_{\text{True}} + P_{\text{False}})(N_{\text{True}} + N_{\text{False}})]^{1/2}}} \quad (16)$$

$$\text{Kappa value (K)} = \frac{Z_i - Z_f}{1 - Z_f} \quad (17)$$

$$Z_0 = \frac{(P_{\text{True}} + N_{\text{True}})}{(P_{\text{True}} + P_{\text{False}} + N_{\text{True}} + N_{\text{False}})}$$

$$Z_e = \frac{[(P_{\text{True}} + P_{\text{False}}) \times (P_{\text{True}} + N_{\text{False}}) + (N_{\text{True}} + N_{\text{False}}) \times (P_{\text{False}} + N_{\text{True}})]}{((P_{\text{True}} + P_{\text{False}} + N_{\text{True}} + N_{\text{False}})^2)}$$

where:

$P_{\text{True}}$  = true positive,

$P_{\text{False}}$  = false positive

$N_{\text{False}}$  = false negative

$N_{\text{True}}$  = true negative

The results obtained from both the models are analyzed using the above performance parameters and also shown in Table 3.



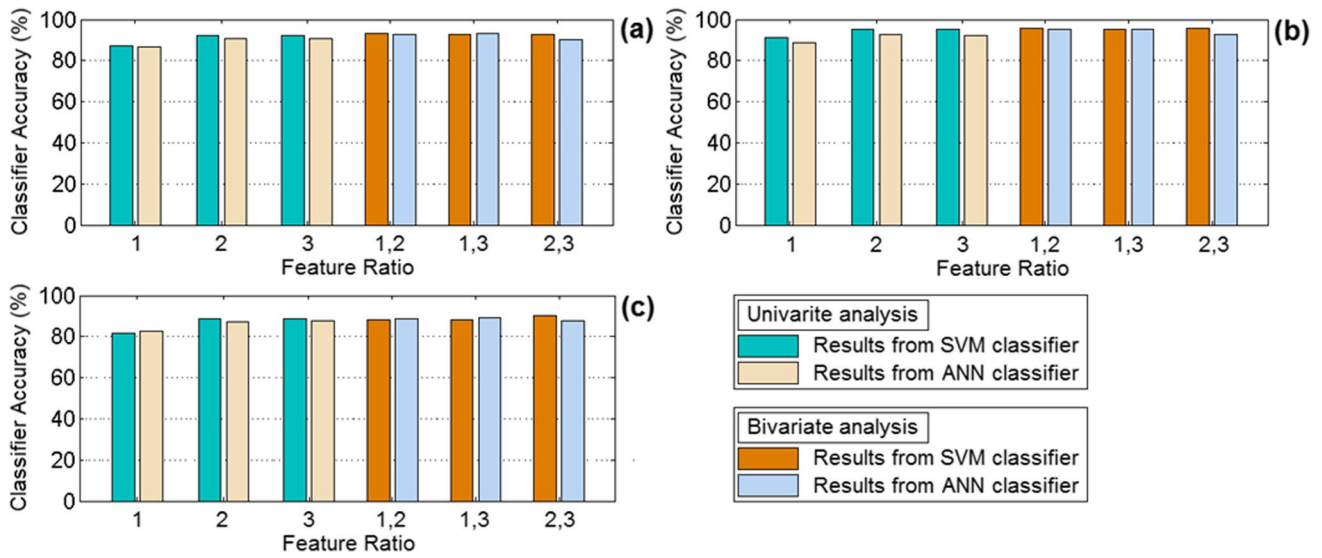


Fig. 12 A comparative analysis of (a) average, (b) maximum, and (c) minimum accuracy obtained from the SVM and ANN classifiers

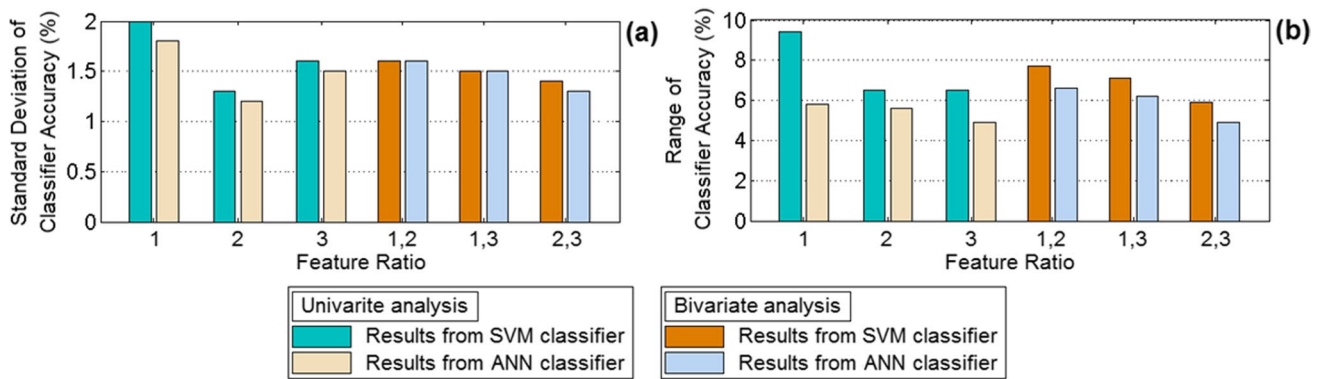


Fig. 13 A comparative analysis of the (a) standard deviation of accuracy outcomes from the mean accuracy level, and (b) range of classifier accuracy obtained from the SVM and ANN classifiers

### Discussion

The proposed work is based on analyzing amla samples of different qualities for the determination of the edibility of the samples. The major highlights of the proposed work are illustrated below.

One of the major highlights of the work is that it eliminates the requirement of capturing images of amla samples following any sort of uniform protocol, such as capturing images from any particular angle or from a certain fixed distance. This is because the amla fruits are close to spherical in shape, and hence, images captured from almost any angle would mostly identify the smoothness of the shape of the *Good* samples and the different superficial

irregularities of the *Deteriorated* samples. This makes the proposed algorithm more generalized in terms of image capturing, even using smartphones. This would help in wide applicability of the model and ensure robustness of the same, especially using smartphones for capturing the images.

In this work, we have used the ratio of the minimum to a maximum distance of the peripheral surface of the samples from the centroid as well as we have also analyzed the ratio of standard division to the minimum value of these peripheral distance values of any particular sample. Hence, it also eliminates the requirement of taking snapshots of the samples from any particular distance or angle. In other words, even if the sample image is small or large, the proposed

**Table 3** Performance parameters obtained from both the models

Classifica- tion model	Feature Ratio used	Accuracy	Precision	Sensitivity	Quality measure	Intersection of overall union	Specificity	Negative pre- dictive value	False posi- tive rate	False nega- tive rate	Mathew correlation	Kappa value
PCA	1	91.18	89.41	92.68	91.02	83.52	89.77	92.94	10.2	7.317	0.82	0.82
	2	95.29	96.47	94.25	95.35	91.11	96.39	94.12	3.61	5.747	0.91	0.91
	3	95.29	95.29	95.29	95.29	91.01	95.29	95.29	4.71	4.706	0.91	0.91
	1, 2	95.88	94.12	97.56	95.81	91.95	94.32	97.65	5.68	2.439	0.92	0.92
	1, 3	95.29	95.29	95.29	95.29	91.01	95.29	95.29	4.71	4.706	0.91	0.91
	2, 3	95.88	96.47	95.35	95.91	92.13	96.43	95.29	3.57	4.651	0.92	0.92
ANN	1	88.53	86.59	91.18	88.83	79.9	85.88	90.68	14.1	8.824	0.77	0.77
	2	92.94	93.98	91.76	92.86	86.67	94.12	91.95	5.88	8.235	0.86	0.86
	3	92.35	94.44	90	92.17	85.47	94.71	90.45	5.29	10	0.85	0.85
	1, 2	95.29	95.29	95.29	95.29	91.01	95.29	95.29	4.71	4.706	0.91	0.91
	1, 3	95.29	94.77	95.88	95.32	91.06	94.71	95.83	5.29	4.118	0.91	0.91
	2, 3	92.65	91.91	93.53	92.71	86.41	91.76	93.41	8.24	6.471	0.85	0.85
	1, 2, 3	94.12	94.64	93.53	94.08	88.83	94.71	93.6	5.29	6.471	0.88	0.88

method of ratio analysis would generalize these differences within appreciable limits. The above two features make the proposed algorithm more generalized as well as robust in terms of image capturing from different angles and distances. These qualities of a classifier are very much required as it is impractical for a person or the automation system which would take the sample images to follow identical protocol every time regarding the angle of the image as well as distance while capturing the images. Hence, the proposed classifier has good quality of robustness as well as practical applicability.

Apart from these features, the proposed work uses the “Canny” edge detection method which is already an established edge detection algorithm. The application of this edge detector identifies the edges in the samples which are very much essential for the work. Apart from that, we have applied the “ConvexHull” analysis on the edge-detected images to extract only the peripheral surface of the samples which are the only requirement for this proposed work. The application of this technique identifies the surface very accurately, thereby helping in accurate estimation of the distance of the surface edge points from the centroid.

The proposed work is light in computation as this incorporates only the edge detection model, followed by validation of the classified features using SVM and ANN methodologies. Hence, this low computational feature enables the proposed model to be applied even on the low memory devices, as well as enables fast computation of the results.

The classifier accuracy obtained using the two models is very high. The average accuracy of classification using the SVM and ANN models exceeds 90% for both the models, considering almost all the ratio features, either in univariate or bivariate mode. The peak accuracy exceeds 95% in both the models using some of the selected feature or feature pairs. This level of accuracy itself is very high when compared to some of the other contemporary schemes. This higher accuracy of classification combined with the robustness of the system makes the proposed algorithm very useful, especially for the detection of freshness of spherical fruit samples like that of amla.

Another very important feature of the work is that the images analyzed here are captured using smartphones only. It is also established by the work that the angles of the images as well as the distance of capturing the same does not majorly affect the classification process. Besides, the low computational burden of the method makes the algorithm suitable for application in low memory devices as well. All these features altogether make the proposed algorithm to be implemented on a very handful device like smartphones using application-based software, especially considering the fact that the images are itself captured in

the same device. This would influence a wide application of the proposed classifier.

## Conclusion

The proposed work is an attempt to develop an accurate freshness detection model for quality assessment of amla samples. In this work, we have analyzed the shape of the samples, which tend to deteriorate progressively with time. The peripheral surface of the samples are detected using Canny edge detection scheme, and these edges are analyzed for identifying the non-uniformity of the surface smoothness, which normally creep into the *Deteriorated* samples. Support vector machine (SVM) and artificial neural network (ANN) are applied further to develop two accurate classifier models, which are able to detect the *Deteriorated* samples with more than 95% peak accuracy level. Besides, ease of capturing the images using smartphones and without following any fixed protocol regarding the angle of capturing images, or the distance from the sample, makes the model more robust. Thus, low computational analysis, high accuracy, and increased robustness make the proposed algorithm suitable for implementation in real-time applications, especially in smartphone-based applications.

**Acknowledgements** We acknowledge the authority, staff, and students of Malda polytechnic, Malda, to being with us throughout the study.

**Funding** Thanks to GAIN (Axencia Galega de Innovación) for supporting this review (grant number IN607A2019/01).

**Availability of Data and Material** All the data used in the manuscript are available in the tables and figures.

**Code Availability** Not applicable.

## Declarations

**Ethics Approval** Not applicable.

**Consent to Participate** All authors have given their full consent to participate.

**Consent for Publication** All authors have given their full consent for publication.

**Conflict of Interest** Tanmay Sarkar declares that he has no conflict of interest. Alok Mukherjee declares that he has no conflict of interest. Kingshuk Chatterjee declares that he has no conflict of interest. Vladimir Ermolaev declares that he has no conflict of interest. Dmitry Piotrovsky declares that he has no conflict of interest. Kristina Vlasova declares that she has no conflict of interest. Mohammad Ali Shariati declares that he has no conflict of interest. Paulo E. S. Munekata de-

clares that he has no conflict of interest. Jose M. Lorenzo declares that he has no conflict of interest.

## References

- Adebo OA, Molelekoa T, Makhuvele R et al (2021) A review on novel non-thermal food processing techniques for mycotoxin reduction. *Int J Food Sci Technol* 56:13–27. <https://doi.org/10.1111/ijfs.14734>
- Angerosa F, Di GL, Vito R, Cumitini S (1996) Sensory evaluation of virgin olive oils by artificial neural network processing of dynamic head-space gas chromatographic data. *J Sci Food Agric* 72:323–328. [https://doi.org/10.1002/\(SICI\)1097-0010\(199611\)72:3%3c323::AID-JSFA662%3e3.0.CO;2-A](https://doi.org/10.1002/(SICI)1097-0010(199611)72:3%3c323::AID-JSFA662%3e3.0.CO;2-A)
- Asif MJ, Shahbaz T, Rizvi STH, Iqbal S (2018) Rice grain identification and quality analysis using image processing based on principal component analysis. In: 2018 International Symposium on Recent Advances in Electrical Engineering (RAEE). pp 1–6. <https://doi.org/10.1109/RAEE.2018.8706891>
- Bhargava A, Bansal A (2020) Automatic detection and grading of multiple fruits by machine learning. *Food Anal Methods* 13:751–761. <https://doi.org/10.1007/s12161-019-01690-6>
- Burkapalli VCPC, Patil (2020) Food image segmentation using edge adaptive based deep-CNNs. *Int J Intell Unmanned Syst* 8:243–252. <https://doi.org/10.1108/IJUS-09-2019-0053>
- Caballero D, Pérez-Palacios T, Caro A et al (2017) Prediction of pork quality parameters by applying fractals and data mining on MRI. *Food Res Int* 99:739–747. <https://doi.org/10.1016/j.foodres.2017.06.048>
- Canny J (1986) A computational approach to edge detection. *IEEE Trans Pattern Anal Mach Intell PAMI-8*:679–698. <https://doi.org/10.1109/TPAMI.1986.4767851>
- Chaphalkar R, Apte KG, Talekar Y et al (2017) Antioxidants of Phyllanthus emblica L bark extract provide hepatoprotection against ethanol-induced hepatic damage: a comparison with silymarin. *Oxid Med Cell Longev* 2017:3876040. <https://doi.org/10.1155/2017/3876040>
- Dang H, Song J, Guo Q (2010) A fruit size detecting and grading system based on image processing. In: 2010 Second International Conference on Intelligent Human-Machine Systems and Cybernetics. pp 83–86. <https://doi.org/10.1109/IHMSC.2010.120>
- Dowlati M, Mohtasebi SS, Omid M et al (2013) Freshness assessment of gilthead sea bream (*Sparus aurata*) by machine vision based on gill and eye color changes. *J Food Eng* 119:277–287. <https://doi.org/10.1016/j.jfoodeng.2013.05.023>
- Dutta Gupta S, Pattanayak AK (2017) Intelligent image analysis (IIA) using artificial neural network (ANN) for non-invasive estimation of chlorophyll content in micropropagated plants of potato. *Vitr Cell Dev Biol - Plant* 53:520–526. <https://doi.org/10.1007/s11627-017-9825-6>
- Gago J, Landín M, Gallego P (2010) Strengths of artificial neural networks in modeling complex plant processes. *Plant Signal Behav* 5:743–745. <https://doi.org/10.4161/psb.5.6.11702>
- Gaikwad B, Manza R (2012) Use of edge detection operators for agriculture video scene feature extraction from mango fruits. *Adv Comput Res* 4:50–53
- Gantait S, Mahanta M, Bera S, Verma SK (2021) Advances in biotechnology of *Emblica officinalis* Gaertn. syn. *Phyllanthus emblica* L a nutraceuticals-rich fruit tree with multifaceted ethnomedicinal uses. *3 Biotech* 11:62. <https://doi.org/10.1007/s13205-020-02615-5>
- Hetal NP, Jain R, Joshi M (2011) Fruit detection using improved multiple features based algorithm. *Int J Comput Appl* 13:1–5

- Hoang N-D, Nguyen Q-L (2018) Metaheuristic optimized edge detection for recognition of concrete wall cracks: a comparative study on the performances of Roberts, Prewitt, Canny, and Sobel algorithms. *Adv Civ Eng* 2018:7163580. <https://doi.org/10.1155/2018/7163580>
- Hu J, Zhou C, Zhao D et al (2020) A rapid, low-cost deep learning system to classify squid species and evaluate freshness based on digital images. *Fish Res* 221:105376. <https://doi.org/10.1016/j.fishres.2019.105376>
- Hussain A, Pu H, Sun D-W (2018) Innovative nondestructive imaging techniques for ripening and maturity of fruits – a review of recent applications. *Trends Food Sci Technol* 72:144–152. <https://doi.org/10.1016/j.tifs.2017.12.010>
- Hussain Hassan NM, Nashat AA (2019) New effective techniques for automatic detection and classification of external olive fruits defects based on image processing techniques. *Multidimens Syst Signal Process* 30:571–589. <https://doi.org/10.1007/s11045-018-0573-5>
- Hussein WB, Moaty AA, Hussein MA, Becker T (2011) A novel edge detection method with application to the fat content prediction in marbled meat. *Pattern Recognit* 44:2959–2970. <https://doi.org/10.1016/j.patcog.2011.04.028>
- Kapoor MP, Suzuki K, Derek T et al (2020) Clinical evaluation of *Emblica officinalis* Gatertrn (Amla) in healthy human subjects: health benefits and safety results from a randomized, double-blind, crossover placebo-controlled study. *Contemp Clin Trials Commun* 17:100499. <https://doi.org/10.1016/j.conctc.2019.100499>
- Koyama K, Tanaka M, Cho B-H et al (2021) Predicting sensory evaluation of spinach freshness using machine learning model and digital images. *PLoS One* 16:e0248769
- Limsiroratanana S, Ikeda Y (2005) Detection of fruits in natural background (part 2). *J Japanese Soc Agric Mach* 67:54–60. [https://doi.org/10.11357/jsam1937.67.5\\_54](https://doi.org/10.11357/jsam1937.67.5_54)
- Liu X, Jiang Y, Shen S et al (2015) Comparison of Arrhenius model and artificial neuronal network for the quality prediction of rainbow trout (*Oncorhynchus mykiss*) fillets during storage at different temperatures. *LWT - Food Sci Technol* 60:142–147. <https://doi.org/10.1016/j.lwt.2014.09.030>
- Ma J, Sun D-W, Qu J-H et al (2016) Applications of computer vision for assessing quality of agri-food products: a review of recent research advances. *Crit Rev Food Sci Nutr* 56:113–127. <https://doi.org/10.1080/10408398.2013.873885>
- Mahale B, Korde S (2014) Rice quality analysis using image processing techniques. In: *International Conference for Convergence for Technology-2014*, pp 1–5. <https://doi.org/10.1109/I2CT.2014.7092300>
- Manickavasagan A, Al-Shekaili HN, Thomas G et al (2014) Edge detection features to evaluate hardness of dates using monochrome images. *Food Bioprocess Technol* 7:2251–2258. <https://doi.org/10.1007/s11947-013-1219-0>
- Mendoza F, Aguilera JM (2004) Application of image analysis for classification of ripening bananas. *J Food Sci* 69:E471–E477. <https://doi.org/10.1111/j.1365-2621.2004.tb09932.x>
- Mendoza F, Dejmeck P, Aguilera JM (2007) Colour and image texture analysis in classification of commercial potato chips. *Food Res Int* 40:1146–1154. <https://doi.org/10.1016/j.foodres.2007.06.014>
- Mukherjee A, Chatterjee K, Sarkar T (2022) Entropy-aided assessment of amla (*Emblica officinalis*) quality using principal component analysis *Biointerface*. *Res Appl Chem* 12:2162–2170. <https://doi.org/10.33263/BRIAC122.21622170>
- Mukherjee A, Sarkar T, Chatterjee K (2021) Freshness assessment of Indian gooseberry (*Phyllanthus emblica*) using probabilistic neural network. *J Biosyst Eng*. <https://doi.org/10.1007/s42853-021-00116-8>
- Musoromy Z, Ramalingam S, Bekooy N (2010) Edge detection comparison for license plate detection. In: *2010 11th International Conference on Control Automation Robotics & Vision*. pp 1133–1138. <https://doi.org/10.1109/ICARCV.2010.5707935>
- Mustafa NBA, Fuad NA, Ahmed SK, et al (2008) Image processing of an agriculture produce: determination of size and ripeness of a banana. In: *2008 International Symposium on Information Technology*. pp 1–7. <https://doi.org/10.1109/ITSIM.2008.4631636>
- Narendra V, VHareesh K. (2011) Study and comparison of various image edge detection techniques used in quality inspection and evaluation of agricultural and food products by computer vision. *Int J Agric Biol Eng* 4:83–90
- Navotas IC, Santos CN V, Balderrama EJM, et al (2018) Fish identification and freshness classification through image processing using artificial neural network. *J Eng Appl* 13(18):4912–4922.
- Nga TTK, Pham TV, Tam DM et al (2021) Combining binary particle swarm optimization with support vector machine for enhancing rice varieties classification accuracy. *IEEE Access* 9:66062–66078. <https://doi.org/10.1109/ACCESS.2021.3076130>
- Pedreschi F, León J, Mery D, Moyano P (2006) Development of a computer vision system to measure the color of potato chips. *Food Res Int* 39:1092–1098. <https://doi.org/10.1016/j.foodres.2006.03.009>
- Péneau S, Brockhoff PB, Escher F, Nuessli J (2007) A comprehensive approach to evaluate the freshness of strawberries and carrots. *Postharvest Biol Technol* 45:20–29. <https://doi.org/10.1016/j.postharvbio.2007.02.001>
- Pratibha N, Hemlata M, Krunali M (2017) Analysis and identification of rice granules using image processing and neural network. *Int J Electron Commun* 10:25–33.
- Priyadumkol J, Kittichaikarn C, Thainimit S (2017) Crack detection on unwashed eggs using image processing. *J Food Eng* 209:76–82. <https://doi.org/10.1016/j.jfoodeng.2017.04.015>
- Przybylak A, Boniecki P, Koszela K et al (2016) Estimation of intramuscular level of marbling among Whiteheaded Mutton Sheep lambs. *J Food Eng* 168:199–204. <https://doi.org/10.1016/j.jfoodeng.2015.07.035>
- Rabby MKM, Chowdhury B, Kim JH (2018) A modified canny edge detection algorithm for fruit detection & classification. In: *2018 10th International Conference on Electrical and Computer Engineering (ICECE)*. pp 237–240. <https://doi.org/10.1109/ICECE.2018.8636811>
- Sanahuja S, Fédou M, Briesen H (2018) Classification of puffed snacks freshness based on crispiness-related mechanical and acoustical properties. *J Food Eng* 226:53–64. <https://doi.org/10.1016/j.jfoodeng.2017.12.013>
- Sarkar T, Mukherjee A, Chatterjee K (2021a) Supervised learning aided multiple feature analysis for freshness class detection of Indian gooseberry (*Phyllanthus emblica*). *J Inst Eng Ser A*. <https://doi.org/10.1007/s40030-021-00585-2>
- Sarkar T, Saha S, Saluddin M, Chakraborty R (2021b) Drying kinetics, Fourier-transform infrared spectroscopy analysis and sensory evaluation of sun, hot-air, microwave and freeze dried mango leather. *J Microbiol Biotechnol Food Sci* 10:1–7
- Sarkar T, Salauddin M, Pati S, et al (2021c) The fuzzy cognitive map-based shelf-life modelling for food storage. *Food Anal Methods*. <https://doi.org/10.1007/s12161-021-02147-5>
- Satone M, Diwakar S, Joshi V (2017) Automatic bruise detection in fruits using thermal images. *Int J Adv Res Comput Sci Soft Eng* 7:727–732. <http://doi.org/10.23956/ijarcse/SV7I5/0116>
- Siswanto J, Prabuwo AS, Abdullah A, Idrus B (2015) Automatic image segmentation using sobel operator and k-means clustering: a case study in volume measurement system for food products. In: *2015 International Conference on Science in Information Technology (ICSITech)*. pp 13–18. <https://doi.org/10.1109/ICSITech.2015.7407769>
- Suktanarak S, Teerachaichayut S (2017) Non-destructive quality assessment of hens' eggs using hyperspectral images. *J Food Eng* 215:97–103. <https://doi.org/10.1016/j.jfoodeng.2017.07.008>

- Thendral R, Suhasini A, Senthil N (2014) A comparative analysis of edge and color based segmentation for orange fruit recognition. In: 2014 International Conference on Communication and Signal Processing. pp 463–466. <https://doi.org/10.1109/ICCSP.2014.6949884>
- Uddin MS, Al MA, Hossain MS et al (2016) Exploring the effect of *Phyllanthus emblica* L. on cognitive performance, brain antioxidant markers and acetylcholinesterase activity in rats: promising natural gift for the mitigation of Alzheimer's disease. *Ann Neurosci* 23:218–229. <https://doi.org/10.1159/000449482>
- Wada Y, Tsuzuki D, Kobayashi N et al (2007) Visual illusion in mass estimation of cut food. *Appetite* 49:183–190. <https://doi.org/10.1016/j.appet.2007.01.009>
- Waliyansyah RR, Hasbullah UHA (2021) Comparison of tree method, support vector machine, naïve Bayes, and logistic regression on coffee bean image. *Emit Int J Eng Technol* 9:126–136. <https://doi.org/10.24003/emitter.v9i1.536>
- Zhu L, Spachos P (2021) Support vector machine and YOLO for a mobile food grading system. *Internet of Things* 13:100359. <https://doi.org/10.1016/j.iot.2021.100359>
- Zhu H, Yang L, Fei J et al (2021) Recognition of carrot appearance quality based on deep feature and support vector machine. *Comput Electron Agric* 186:106185. <https://doi.org/10.1016/j.compag.2021.106185>
- Sarkar T, Mukherjee A, Chatterjee K, Shariati, MA et al (2021d) Comparative Analysis of Statistical and Supervised Learning Models for Freshness Assessment of Oyster Mushrooms. *Food Anal Methods* <https://doi.org/10.1007/s12161-021-02161-7>

**Publisher's Note** Springer Nature remains neutral with regard to jurisdictional claims in published maps and institutional affiliations.